Electronic structure of $Na_xCu_{1-x}In_5S_8$ compounds: X-ray photoemission spectroscopy study and band structure calculations

Catherine Guillot-Deudon, Sylvie Harel, Arezki Mokrani, Alain Lafond, Nicolas Barreau, Vincent Fernandez, and John Kessler

Institut des Matériaux Jean Rouxel (IMN), Université de Nantes, CNRS, 2 rue de la Houssinière, BP 32229, 44322 Nantes Cedex 03, France

(Received 7 April 2008; published 3 December 2008)

The aim of the present work is to complete a preliminary study concerning the electronic band structure investigations of $Na_xCu_{1-x}In_5S_8$ compounds with $0 \leq x \leq 1$, which are expected to be formed at the $Cu(In,Ga)Se_2/In_2S_3$ interface. The band structure calculations demonstrate that for the compounds containing both Na and Cu, as the Cu content increases the band gap tends to decrease, and x-ray photoemission spectroscopy measurements show that this variation is mainly due to valence-band-maximum shift along the solid solution. The band gap strongly depends on the nature of the monovalent cation, and the band structure calculations demonstrate that the *d* electrons of copper are responsible for the shift of the valence band. In addition, it is worth noting that the Cu-containing compounds have indirect gaps.

DOI: 10.1103/PhysRevB.78.235201 PACS number(s): 71.15.Mb, 71.20.Nr, 82.80.Pv

I. INTRODUCTION

Thin-film solar cells based on $CuIn_{1-x}Ga_xSe_2$ (CIGSe) absorber materials have reached efficiencies close to 20%.[1] The standard devices consist of Mo/CIGSe/CdS/ZnO structures deposited on soda lime glass substrates. Although the cadmium sulfide (CdS) buffer layer deposited by chemical bath (CBD) is a very well-adapted junction partner for standard CIGSe ($x \sim 0.2-0.3$) due to the cadmium toxicity; it would be preferable that it be substituted by a cadmium-free material. This issue is among the challenges of the CIGSe solar cell community since the end of the 1990s.[2,3] A general conclusion of these investigations is that the most relevant materials are zinc-based semiconductors [i.e., (Zn,Mg)O (Ref. 4) and Zn(S,O) (Refs. 5 and 6)] and indium sulfide (In_2S_3).[7,8] Basically, an efficient buffer layer should minimize carrier recombination at the absorber or buffer layer interface. With this aim, at least two conditions are recommended:[9] (i) that the Fermi-level be close to the conduction band at the interface (inverted surface), which can be achieved by a highly doped buffer layer or appropriated interface charges and (ii) that there be no recombination barrier reduction, meaning that there be no interface band cliff. It thus appear that both the electrical properties and the band structure of the materials at the interface are very important for the device performance.

A particularity of the CIGSe/indium sulfide interface is that copper and sodium diffuse from the absorber layer into the buffer layer. These diffusions occur either during the indium sulfide deposition or during the cells postfabrication annealing. The absorber or buffer material transition is therefore graded contrarily to the abrupt transition observed in the case of zinc-based buffer layers. It has been observed that the compounds formed at the CIGSe/indium sulfide interface have a crystalline structure derived from that of indium sulfide,[10,11] independently of the copper and sodium migration. Several articles were already devoted to these interfacial compounds,[12–15] and our assumption is that these materials result from insertion or substitution mechanism allowed by the specific In_2S_3 crystalline structure. The indium sulfide indeed crystallizes in a cationic-deficient spinel-like structure with the formulation $[In_{16}]_{Oh}[In_{16/3}[]_{8/3}]_{Td}S_{32}$, where [] represents the vacant sites, Oh and Td index the octahedral and tetrahedral sites, respectively. Transmission electron microscopy studies lead to the conclusion that when copper and/or sodium are introduced within the In_2S_3, mechanism also involved while copper and sodium diffuse from the CIGSe into the In_2S_3, the structure thus achieved can be described as $[In_{16}]_{Oh}[In_{(16-\alpha)/3}Na_{\alpha}[]_{(8-2\alpha)/3}]_{Td}S_{32}(\alpha \leq 4)$.[16] This formulation assumes that two-thirds of the introduced atoms effectively fill cationic vacancies (i.e., insertion), the other third is being substituted to indium in order to keep electroneutrality (i.e., substitution). The limit composition, i.e., $\alpha=4$, corresponds to the MIn_5S_8 phase (M:Cu and/or Na). Assuming that these compounds are effectively formed at the $CIGSe/In_2S_3$ interface, progress in the device operation understanding requires improved knowledge of these materials properties.

The purpose of the present study is to determine the band structure evolution of $(Na_xCu_{1-x})In_5S_8$ when x varies from 0 to 1. With this aim, the crystalline parameters of powders corresponding to different x values have been accurately evaluated. Then, with the help of this information, the electronic band structure of each composition has been determined using the *ab initio* tight-binding linear muffin-tin orbital (TBLMTO) method. The correlation between the results of these calculations and the x-ray photoelectron spectroscopy (XPS) measurements is used to discuss the influence of copper and sodium diffusions on the performance of solar cells based on $CIGSe/In_2S_3$ junction.

II. EXPERIMENTAL DETAILS

A. Preparation and XRD characterization

A previous paper[14] reports on the synthesis and the existence of the solid solution $Na_xCu_{1-x}In_5S_8$ with $0 \leq x \leq 1$. For the present study all experiments were carried out in a dry

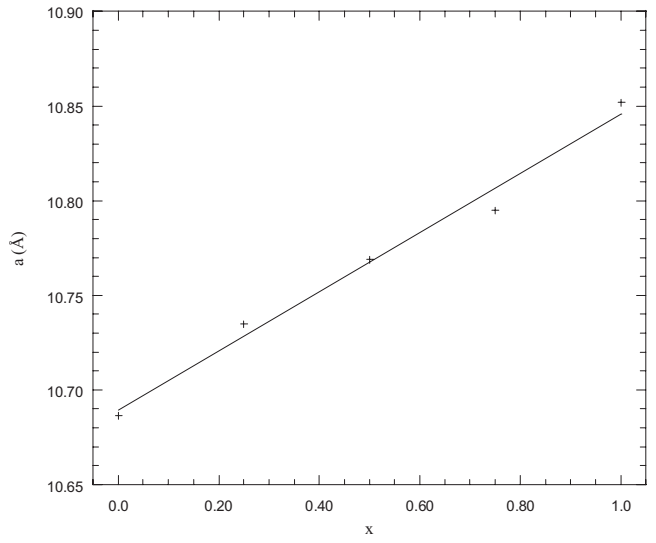

FIG. 1. Evolution of the cubic unit-cell parameter *a* along the solid solution.

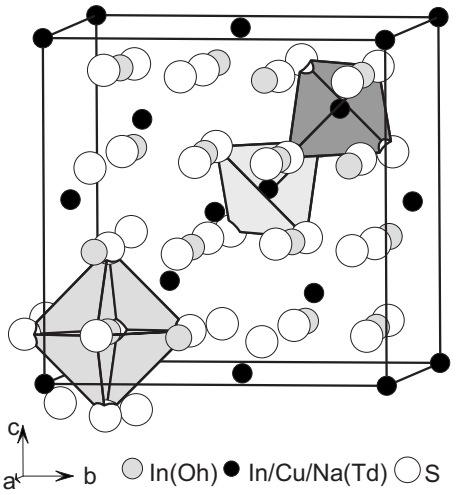

FIG. 2. Structure of the $Na_xCu_{1-x}In_5S_8$ compounds. An example of the two types of tetrahedral and octahedral sites are represented in the unit cell.

box under Ar in order as much as possible to avoid oxygen contamination. The samples were synthesized by solid-state reaction route. The homogeneity and the composition of the powders were assessed from the powder x-ray diffraction (XRD) technique. The full pattern matching refinements were carried out with the help of the programs FULLPROF (Ref. 17) and WINPLOTR.[18] Figure 1 presents the variation in the cubic unit-cell parameter *a* along the solid solution $Na_xCu_{1-x}In_5S_8$. Contraction of about 1.5% of the lattice parameter is observed from $NaIn_5S_8$ to $Cu_1In_5S_8$.

B. XPS measurements

X-ray photoemission spectra were performed on a Kratos AXIS Ultra spectrometer using a monochromatic Al K_α x-ray source (1486.6 eV). The x-ray source runs at 150 W. The base pressure in the analysis chamber was 10^{-8} Pa and the analyzed area was 700×300 μm^2. The hemispherical analyzer was used in constant analyzer energy (CAE) mode for all spectra. The pass energy was 160 eV for wide-scan spectra and 20 eV for narrow scan and valence band (VB). The energy scale was calibrated using Au $4f_{7/2}$ at 83.97 eV and Cu $2p_{3/2}$ peaks at 932.63 eV measured from sputter-cleaned Au and Cu films.[19] The overall energy resolution, as determined using the Fermi edge of an Ag reference, was 0.47 ± 0.03 eV at 20 eV pass energy.

The samples were ground and pressed into 6-mm-diameter pellets and mounted on double-sided carbon tape on an aluminium plate and were quickly transferred from the glove box to the XPS spectrometer. Only one of the compounds ($Na_{0.25}Cu_{0.75}In_5S_8$) has presented poor compressibility behavior and charge effects occurred during spectra recording. For this reason, it was necessary to neutralize the surface charge with an electron flood gun. The charge neutralizer induces polarization of the surface of about $+2.2$ V ±0.3 V.

III. STRUCTURAL DESCRIPTION

The $Na_xCu_{1-x}In_5S_8$ compounds belong to the solid solution $NaIn_5S_8$-$CuIn_5S_8$ with a cubic structure related to that of the cation-deficient spinel-like compound In_2S_3, resulting from the insertion or substitution mechanism described in the introduction. The detailed structural description can be found elsewhere.[14,20] Here we just recalled that indium, sodium, and copper atoms are statistically distributed in the two kinds of tetrahedral sites, Td1 and Td2, referenced as to be the 4*a* and 4*c* of the space group *F*-43*m*. The unit cell is sketched in Fig. 2 and the atomic positions deduced from the structure determination of a single crystal with *x* close to 0.5 are given in Table I. These atomic positions are used for the electronic

TABLE I. Atomic positions in $Na_xCu_{1-x}In_5S_8$ according to the structure determination from a single crystal of composition close to $x=0.5$ (Ref. 14). Space group *F*-43*m* and $a=10.7692(3)$Å.

Wyckoff position (type of cationic site)	Atom	*x*	*y*	*z*
4a (Td1[a])	In/Na/Cu	0	0	0
4c (Td2[a])	In/Na/Cu	1/4	1/4	1/4
16e (Oh[a])	In	0.6268	0.6268	0.6268
16e	S1	0.3821	0.3821	0.3821
16e	S2	0.8682	0.8682	0.8682

[a]Td1 and Td2=tetrahedral sites and Oh=octahedral site.

band structure calculations presented below.

IV. COMPUTATIONAL APPROACH

In order to better understand the band structure of the $Na_xCu_{1-x}In_5S_8$ compounds, *ab initio* electronic structure calculations were performed using density-functional theory. The scalar-relativistic tight-binding linear muffin-tin orbital method was used with the atomic spheres' approximation (TB-LMTO-ASA).[21–23] The von Barth–Hedin local exchange correlation potential was used with Langreth-Mehl-Hu nonlocal correction.[24,25] The eigenvalues and eigenvectors were determined using the tetrahedron technique with an increasing number in k points in the irreducible Brillouin zone (BZ); until final convergence is obtained ($14\times14\times14$ k points are used in these calculations). This approach, based on the local spin-density approximation (LDA),[24] was used in our previous theoretical work[26] devoted to comparative study of the gap evolution under lattice compression of In_2X_3 (X =O,S,Se,Te). Although the LDA gives a correct ground state in term of insulating or metallic behavior,[27] it fails usually to reproduce quantitatively the energy-band gaps. However, in this work we focus on the band structure modification and the relative variations of the gap and not in the quantitative evaluation. This approach seems to be reasonable to describe the band structure of $Na_xCu_{1-x}In_5S_8$ compounds and to determine the band-gap evolution for different atomic configurations corresponding to different values of x.

In our calculations we used the crystallographic cubic unit cell (Fig. 2) containing 56 atoms: 32 S, 20 In, and 4 M (M =Cu,Na). This unit cell presents 16 octahedral sites occupied by the In and 8 tetrahedral sites occupied by In and the monovalent atoms Na and Cu. The atomic configurations, corresponding to the different distributions of the In and M atoms on the tetrahedral sites (Td1 and Td2) subnet for different relative compositions were investigated. In this numerical approach the first step is to find the most stable configuration among all possible configurations obtained by different ways to fill tetrahedral sites. Three configurations were considered. The first one is obtained by filling all the Td1 sites by In and Td2 by M (Cu or Na) atoms. The second consists of a nonsymmetrical filling placing one atom M and three In on the same type of tetrahedral site and 3 M and one In on the other type of tetrahedral site. The third configuration corresponds to a symmetrical filling, 2 M and 2 In on each type of tetrahedral site. The total-energy calculations clearly show that the latter configuration is the most stable, which agrees perfectly with the single-crystal structural resolution (statistical distribution of 2 In and 2 M on Td1 and Td2). Thus this configuration was used for this work. In the second step, the lattice parameters of the studied compounds were optimized. The obtained values are about 10.84 Å for $CuIn_5S_8$ and 10.95 Å in the case of $NaIn_5S_8$. These results are in good agreement with the experimental observations showing also a small lattice expansion when Na content increases (Fig. 1).

In order to properly interpret the meaning of the valence-band XPS measurements, the total and partial densities of states (DOSs) of each type of atom were calculated. All different contributions to the valence band will be discussed in detail in the following sections to interpret the XPS results and understand the evolution of the band gap of these photovoltaic compounds.

V. RESULTS AND DISCUSSION

A. Core levels

High-resolution spectra of S $2p$, In $3d$, Na $1s$, and/or Cu $2p_{3/2}$ core levels were acquired for all of the compounds. The peaks relative to the C $1s$ and O $1s$ levels were also investigated in order to check the cleanliness of the samples as surface contamination can hinder the reliability of the VB spectra. It can be deduced from the low C $1s$/In $3d_{5/2}$ and O $1s$/In $3d_{5/2}$ intensity ratio and low sensitivity factor (σ) of the C $2p$ relative to the In $5p$ and Cu $3d$ (Ref. 28) that the sample contamination contribution to the valence band is very low and similar between samples. Therefore it is assumed that its impact on the valence-band shape change can be neglected.

For all values of x, the In $3d$ doublet is well resolved with the usual $3d_{5/2}/3d_{3/2}$ intensity ratio of 3/2, indicating a single contribution. Moreover, the shape of the In $3d$ doublets remains similar with varying x suggesting that this core level is not affected by the varying composition. In order to determine the In $3d_{5/2}$ peak position taking into account possible charge effects, the spectra were slightly shifted to the position of the C $1s$ peak at 284.8 eV. The In $3d_{5/2}$ position appeared independent of x at 444.2 eV $\pm$ 0.1 eV, binding energy very close to that of In_2S_3 (444.3 eV).[29]

B. Valence band

As the position of the valence-band maximum (VBM) is of major interest for the photovoltaic compounds we focused our attention on its evolution within the series. The valence-band spectra were measured between −4 and 24 eV in order to access the In $4d$ level, which is used as energy reference. This band behaves as an outer core state and does not participate in the bonding.[30–32] The position of the In $4d_{5/2}$ is 18.5 $\pm$ 0.1 eV for all compounds. Likewise in order to compare the valence-band shapes, all of the spectra were normalized relatively to In $4d$ core level. The obtained XPS valence band for all of the $Na_xCu_{1-x}In_5S_8$ are plotted in the Fig. 3. One can notice that the intensity ratio between the higher intensity of the valence band located at 3.6 eV corresponding to the sample and the intensity at 10 eV due to the pollution and secondary electron is about 6. This high value indicates the cleanliness of the samples and consequently the reliability of the measurements.

If we first focus our attention on the VBM position, one can clearly observe its shift toward higher energies as x is increased. This result corroborates the previous study.[15] Second, the valence band appears to be composed of two main contributions for all values of x. The broader one in the energy range (1–7 eV) is labeled region A, and the narrower one, labeled region B, is in the energy range (7–9 eV). The shape as well as the position of region B appear to be independent of x, whereas the region A strongly varies from

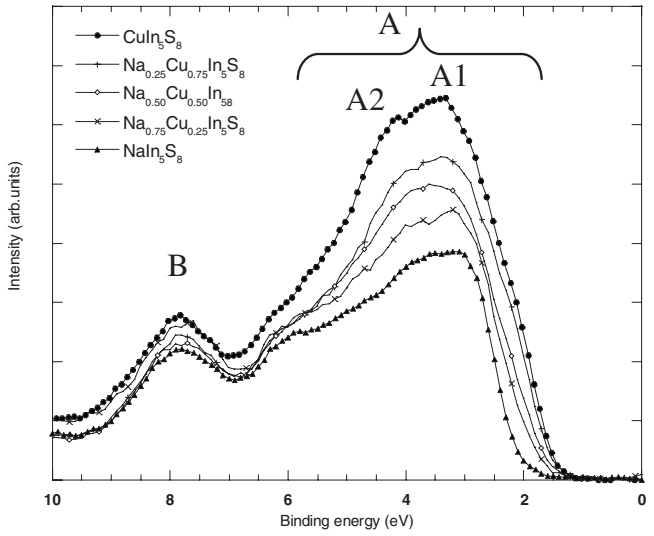

FIG. 3. XPS valence band of $NaIn_5S_8$, $Na_{0.75}Cu_{0.25}In_5S_8$, $Na_{0.50}Cu_{0.50}In_5S_8$, $Na_{0.25}Cu_{0.75}In_5S_8$, and $CuIn_5S_8$.

$NaIn_5S_8$ to $CuIn_5S_8$. There is a clear increase in the electronic density located at the top of the valence band. Moreover, one observes that the intensity of the broad band A increases with Cu content as well. As it is convenient to discuss the DOS structure in terms of the same features identified in the calculated valence band, two subbands labeled A1 and A2 will be distinguished in the A region. In order to examine the distribution of the states within the valence band and interpret this $Na_xCu_{1-x}In_5S_8$ experimental valence-band spectra evolution with x, the total and partial DOS were calculated in the energy range (−20–5 eV). The results of these investigations are plotted in Figs. 4 and 5. The highest occupied state is taken as zero energy. The LDA approach underestimates the calculated bandwidths; therefore, the comparison of the experimental and theoretical results will remain qualitative.

On the top panel of Fig. 4 the total DOS for $NaIn_5S_8$ [Fig. 4(a)] and $CuIn_5S_8$ [Fig. 4(e)], where zero energy corresponds to the top of the valence band, are reported. In order to ease the comparison with the experimental XPS results (Fig. 3), similar labels A1, A2, and B were chosen to indicate the main regions in the valence band. Considering the total DOS, the main difference between $NaIn_5S_8$ and $CuIn_5S_8$ appears at the top part of the valence band where a sharp peak (A1) is observed for $CuIn_5S_8$. This peak is clearly identified as the contribution of Cu d states illustrated by the calculated 3d partial DOS plotted in Fig. 4(h). Because of this feature (A1), A2 and B regions shift toward the higher binding energy in the calculated DOS. One can notice that in these A2 and B regions, Na and Cu orbitals have a negligible contribution compared to In and S states [Figs. 4(d) and 4(h)]; this is the reason why these regions keep the same structure and the same energy width. These results can be compared to previous studies on In_2S_3.[26,31,32] The In_2S_3 XPS VB shows the same structures than the presently studied $NaIn_5S_8$, and the band structure calculations lead to the same assignments for both compounds.

In order to illustrate the electronic structure evolution with increasing x, the $Na_xCu_{1-x}In_5S_8$ total DOS when $x=0$, 0.25, 0.5, 0.75, and 1 are displayed in Fig. 5. When $x<1$, i.e., the compound contains copper, the Cu 3d states (A1) appear at the top of the valence band close to the A2 and B bands, and this A1 structure intensity increases with increasing copper content [see Figs. 5(b)–5(e)]. In the case of $NaIn_5S_8$ [Fig. 5(a)], as the A1 structure does not exist, the A2 mass (band) is located at the top of the VB, taken as zero energy in band structure calculations. Thus the energy scale must be shifted. In Fig. 6 the calibrated total DOS of both the $CuIn_5S_8$ and $NaIn_5S_8$ materials using the In 4d are plotted. After calibration, the $CuIn_5S_8$ VBM is shifted toward the lower binding energies compared to the $NaIn_5S_8$ VBM. It also appears that the B and A2 regions energy positions are not affected. All of these results are in a good agreement with the experimental valence-bands evolution with x. Indeed the XPS experiments (Fig. 3) show that mainly the top of the valence band is affected by the increase in the copper content; the contributions B and A2 appear to be independent of x. One may note that the intensity increase in the A2 peak experimentally observed is due to the A1 peak intensity increase with increasing copper content.

Band structure calculations provide also information on the conduction band as well as the band gap. From the band structure calculations a large band gap is obtained for $NaIn_5S_8$ in comparison to $CuIn_5S_8$ [Figs. 4(a) and 4(e)]. For the $Na_xCu_{1-x}In_5S_8$ compounds containing both Na and Cu, as the Cu content increases the band gap tends to decrease (Fig. 5). These results corroborate the previous study where we had already experimentally shown that the optical band gap of these compounds increases linearly between $x=0$ ($CuIn_5S_8$) and $x=0.75$, whereas for $x=1$ ($NaIn_5S_8$) it was higher than the value expected from a linear behavior. The band gap strongly depends on the nature of the M atom and it is clear that the d electrons of Cu are responsible for the shift of the VB. Indeed the distances between the cationic sites are quite large [d(Td-Oh) ≈ 4.5 Å and d(Td-Td) ≈ 4.7 Å] so the environment of both In (Td) and In (Oh) are only very slightly affected when copper atoms replace sodium. Thus, the contribution of the In atoms to the electronic band structure will remain unchanged within the solid solution.

By means of calculations, we had demonstrated that the Cu-containing compounds have an indirect band gap[15] with conduction bands at almost constant energy level. The copper plays a main role on the evolution of the band gap and consequently on the optical properties.

C. Impact on the performance of the solar cells and concluding remarks

High efficiencies have been achieved by CIGSe-based solar cells buffered with indium sulfide grown by numerous techniques. The correlation between the device performance and the corresponding CIGSe/indium sulfide heterointerface properties has revealed that the amount of copper and sodium atoms diffusing from the absorber into the buffer layer strongly influences the cells electrical parameters.[33] The above presented results corroborate and give insight into the following assumptions.

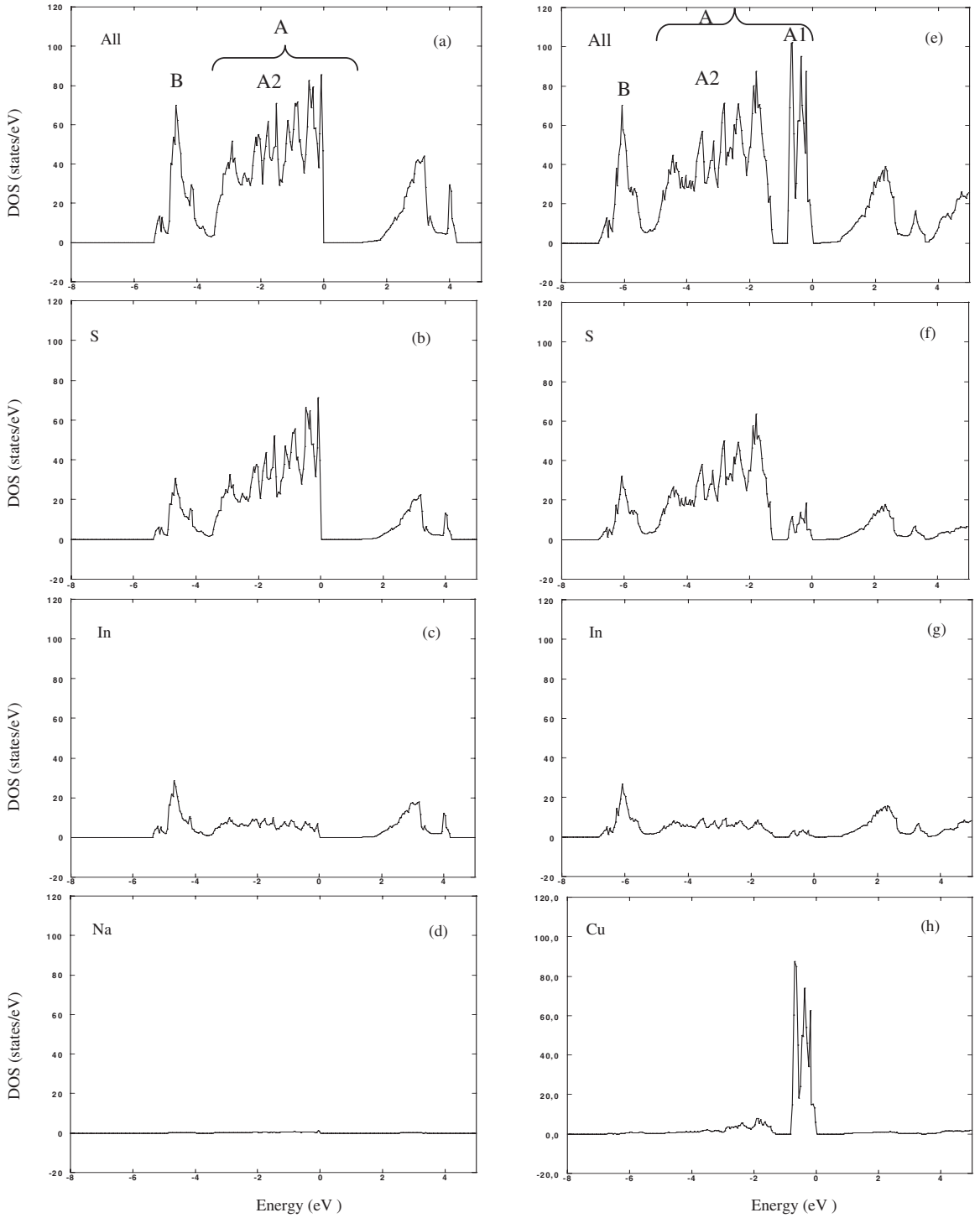

FIG. 4. Total DOS of (a) $NaIn_5S_8$ and (e) $CuIn_5S_8$. Partial DOS of $NaIn_5S_8$; (b) S 3*p*, (c) In total, and (d) Na Partial DOS of $CuIn_5S_8$; (f) S 3*p*, (g) In total, and (h) Cu 3*d*. The top of the valence band is taken as zero energy.

The introduction of copper into the indium sulfide narrows its band gap because of the presence of the Cu 3*d* orbitals at the top of the valence band. In contrast, the presence of sodium widens the indium sulfide band gap mainly by shifting the valence band downward, the conduction band being only slightly moved upward.[15] It thus appears that when both copper and sodium atoms are introduced together, the effect of the sodium is hindered by the presence of the 3*d* orbitals of the copper. This assumption agrees well with the experimental results that the $Na_xCu_{1-x}In_5S_8$ band gap width evolution versus x is linear as long as the material contains copper ($x<1$), whereas the copper-free material ($x=1$) band gap value is off this linear behavior.[14]

Among the remaining questions concerning the indium sulfide buffer layer issue is whether the copper and sodium diffusions are beneficial for the device performance. The

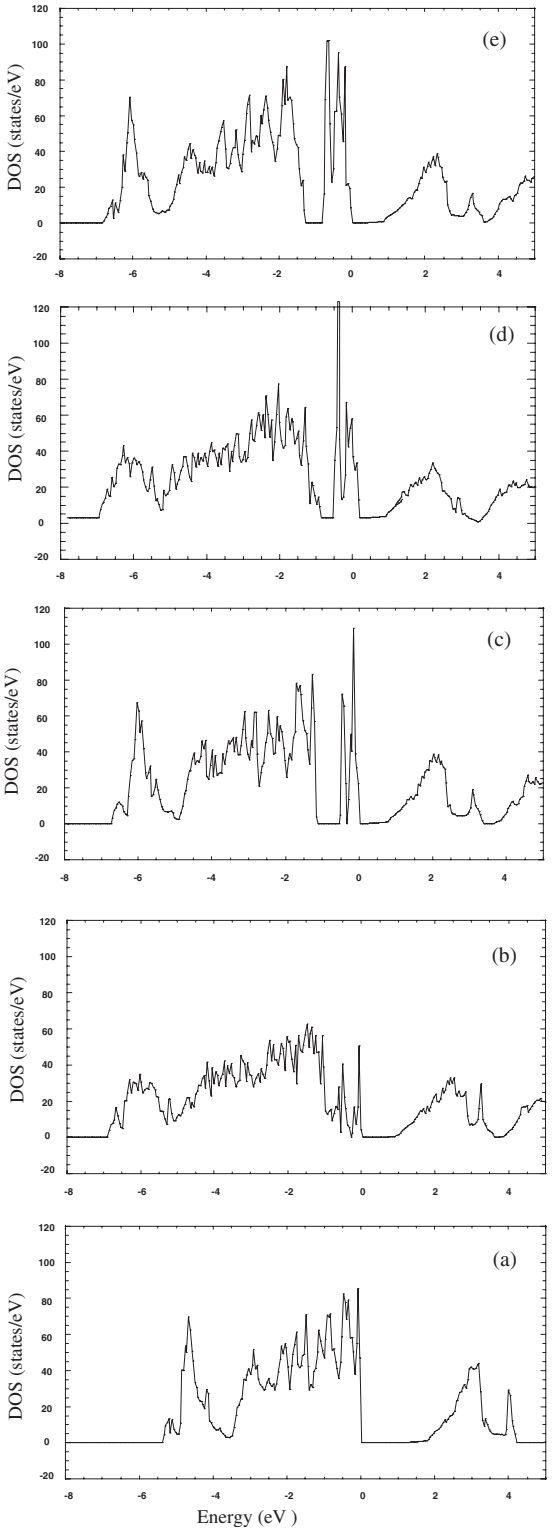

FIG. 5. Total DOS of (a) $NaIn_5S_8$, (b) $Na_{0.75}Cu_{0.25}In_5S_8$, (c) $Na_{0.50}Cu_{0.50}In_5S_8$, (d) $Na_{0.25}Cu_{0.75}In_5S_8$, and (e) $CuIn_5S_8$.

present results suggest that the band structure on the buffer layer side of the CIGSe/In_2S_3 interface is strongly influenced by the copper diffusion, whereas the sodium migration has a lesser impact. Taking into account that the presence of copper shifts the buffer valence-band maximum upward, it also reduces the CIGSe/In_2S_3 interface valence-band offset.

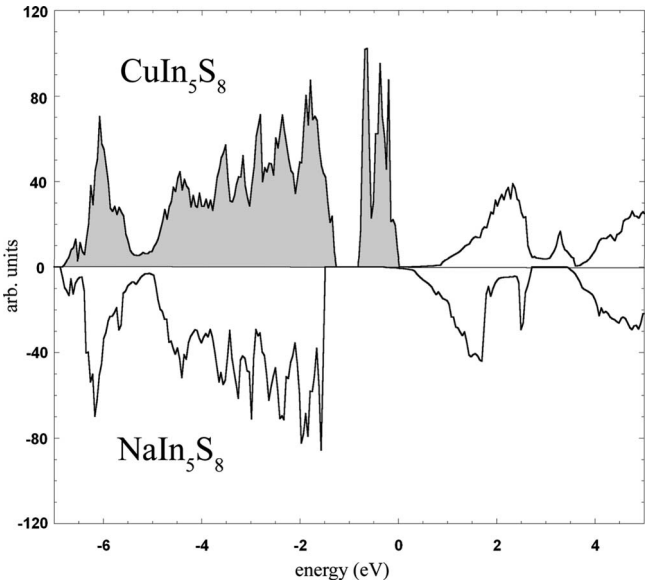

FIG. 6. Total DOS of $NaIn_5S_8$ and $CuIn_5S_8$. The energy scale is calibrated using In 4*d* orbital.

Such a decrease (several tenths of electron volt) is not expected to hinder the device performance as long as the offset is not changed to an onset (i.e., VBM_{buffer} above the $VBM_{absorber}$), a configuration which should lead to low photovoltaic performance. On the other hand, the interface conduction-band structure appears to be not affected by the copper diffusion. Therefore, regardless the changes induced in the CIGSe surface, the effects on the interface band structure of the copper diffusion does not appear to be beneficial for the cells performance.

Although the main effects of sodium on the buffer layer band structure are partly hindered by the presence of copper, a slight influence is nevertheless expected at the CIGSe/In_2S_3 interface conduction-band structure. Such a buffer layer electron affinity decrease, even as low as a few millielectron volt, may strongly impact on the open circuit voltage and fill factor (e.g., conduction-band cliff decrease). Therefore, considering the interface band structure, one can assume that the sodium can be beneficial for the cells performance.

Optically, the nature of the band gap is changed depending on whether the material contains copper or not; the copper-free material has a direct band gap, whereas the presence of copper leads to indirect band gap compounds. This phenomenon can be considered a positive aspect of the copper diffusion; nevertheless, the energy difference between the indirect and the direct absorption thresholds has still not been investigated. This energy difference may moreover also depend on the sodium content of the material, which would make the buffer layer sodium content more important than that of the copper for the short-wavelengths transmission.

Considering only the buffer layer side of the *pn* junction, it therefore seems that the diffusion of copper is less desirable than that of sodium for the device performance. However, the present discussion has only taken into account the band structure and the optical properties of the buffer layer. A final conclusion should not be drawn without considering

the electrical changes due to the presence of copper and sodium. Moreover, the impact of the diffusions on the absorber surface properties should moderate the present conclusions.

VI. CONCLUSION

$Na_xCu_{1-x}In_5S_8$ $(0 \leq x \leq 1)$ compounds are probably formed at the CIGSe/In_2S_3 interface in solar cells. In this paper a detailed investigation of the valence-band structure of these compounds is presented from both XPS measurements and *ab initio* calculations. The XPS investigations have shown that the valence-band maximum position is strongly influenced by the Cu content (i.e., value of x). The combination of these results with the band structure calculations has pointed out the origin of the copper influence. Indeed, the calculations have shown that the Cu $3d$ orbitals appear at the top of valence band and are thus the main culprit of the band gap decrease when Cu content increases. The conclusions of this work are useful in understanding the CIGSe/In_2S_3-based devices operation.

[1] M. A. Contreras, K. Ramanathan, J. AbuShama, F. Hasoon, D. L. Young, B. Egaas, and R. Noufi, Prog. Photovoltaics **13**, 209 (2005).
[2] D. Hariskos, S. Spiering, and M. Powalla, Thin Solid Films **99**, 480 (2005).
[3] S. Siebentritt, Sol. Energy **77**, 767 (2004).
[4] T. Törndahl, C. Platzer-Björkman, J. Kessler, and M. Edoff, Prog. Photovoltaics **15**, 225 (2007).
[5] A. Ennaoui, M. Bär, J. Klaer, T. Kropp, R. Saez-Araoz, and M. C. Lux-Steiner, Prog. Photovoltaics **14**, 499 (2006).
[6] C. Platzer-Björkman, J. Kessler, and L. Stolt, Proceedings of the Third World Conference Photovoltaic Energy, Osaka, 2003 (unpublished).
[7] N. Naghavi, S. Spiering, M. Powalla, B. Cavana, and D. Lincot, Prog. Photovoltaics **11**, 437 (2003).
[8] N. A. Allsop, A. Schönmann, H. J. Muffler, M. Bär, M. C. Lux-Steiner, and C. H. Fisher, Prog. Photovoltaics **13**, 607 (2005).
[9] R. Klenk, Thin Solid Films **387**, 135 (2001).
[10] D. Abou-Ras, D. Rudmann, G. Kostorz, S. Spiering, M. Powalla, and A. N. Tiwari, J. Appl. Phys. **97**, 084908 (2005).
[11] D. Abou-Ras, G. Kostorz, A. Strohm, H. W. Schock, and A. N. Tiwari, J. Appl. Phys. **98**, 123512 (2005).
[12] N. Barreau and J. C. Bernède, Proceedings of the 19th European Photovoltaic Solar Energy Conference, Paris, edited by W. Hoffmann, J.-L. Bal, H. Ossenbrink, W. Palz, and P. Helm, (2004).
[13] N. Barreau, S. Gall, S. Marsillac, J. Kessler, and A. Rockett, Proceedings of the 20th European Photovoltaic Solar Energy Conference and Exhibition, Barcelona, 2005 (unpublished).
[14] N. Barreau, C. Deudon, A. Lafond, S. Gall, and J. Kessler, Sol. Energy Mater. Sol. Cells **90**, 1840 (2006).
[15] A. Lafond, C. Guillot-Deudon, S. Harel, A. Mokrani, N. Barreau, S. Gall, and J. Kessler, Thin Solid Films **515**, 6020 (2007).
[16] N. Barreau, J. C. Bernède, C. Deudon, L. Brohan, and S. Marsillac, J. Cryst. Growth **241**, 4 (2002).
[17] J. Rodriguez-Carjaval, Physica B (Amsterdam) **192**, 55 (1993).
[18] T. Roisnel and J. Rodriguez-Carjaval, Mater. Sci. Forum **378-381**, 118 (2001).
[19] M. P. Seah, I. S. Gilmore, and G. Beamson, Surf. Interface Anal. **26**, 642 (1998).
[20] L. Gastaldi and L. Scaramuzza, Acta Crystallogr., Sect. B: Struct. Crystallogr. Cryst. Chem. **36**, 2751 (1980).
[21] O. K. Andersen and O. Jepsen, Phys. Rev. Lett. **53**, 2571 (1984).
[22] O. K. Andersen, O. Jepsen, and D. Glotzel, Proceedings of the International School of Physics "Enrico Fermi", Amsterdam, 1985 (unpublished).
[23] O. K. Andersen, Z. Pawlowska, and O. Jepsen, Phys. Rev. B **34**, 5253 (1986).
[24] D. C. Langreth and M. J. Mehl, Phys. Rev. B **28**, 1809 (1983).
[25] U. von Barth and L. Hedin, J. Phys. C **5**, 1629 (1972).
[26] R. Robles, A. Vega, and A. Mokrani, Opt. Mater. **17**, 497 (2001).
[27] G. Pari, S. Mathi Jaya, G. Subramoniam, and R. Asokamani, Phys. Rev. B **51**, 16575 (1995).
[28] J. H. Scofield, J. Electron Spectrosc. Relat. Phenom. **8**, 129 (1976).
[29] G. D. Nichols and D. A. Zatko, Inorg. Nucl. Chem. Lett. **15**, 401 (1979).
[30] D. Schmid, M. Ruckh, and H. W. Schock, Appl. Surf. Sci. **103**, 409 (1996).
[31] E. Domashevskaya, V. Terekhov, L. Marshakova, and Y. Ugai, J. Electron Spectrosc. Relat. Phenom. **9**, 261 (1976).
[32] A. Lavrent'ev, N. Safontseva, V. Dubeiko, B. Gabrel'yan, and I. Nikiforov, Phys. Solid State **42**, 2047 (2000).
[33] S. Spiering, A. Eicke, D. Hariskos, M. Powalla, N. Naghavi, and D. Lincot, Thin Solid Films **562**, 451 (2004).